NUMERICAL ANALYSIS OF SLOSHING PROBLEM

Yonghwan Kim

American Bureau of Shipping
Research Department, Houston, TX, USA

Introduction

   Many studies have been reported for the sloshing analysis in liquid containers. One of the major concerns in the marine hydrodynamic field is the accurate prediction of impulsive load on internal structures. During violent sloshing, the sloshing-induced impact load can cause a critical damage on tank structure. Such damage cases have been reported for oil tankers, LNG carriers and bulk carriers. Recently, this problem becomes an important issue in FPSO design.

   Many analytical and experimental studies on sloshing were performed in the 1950's and 1960's for the tank design of space vehicles. In the 1970's and early 1980's, the sloshing problem became an important issue in the design of the liquified natural gas (LNG) carriers. Some numerical methods were applied during this time, and such studies can be found in the works of Faltinsen[2], Bridges[1], Mikelis and et al[5]. Some Japanese researchers have continued the study, and many interesting results have been introduced for the two- and three-dimensional sloshing problems. Recently some computational results using the general-purpose flow simulation programs, like FLOW3D, have reported for the sloshing analysis. However, the application of the general-purpose programs may be not proper for the prediction of impulsive loads, since the typical numerical treatment of wall condition can result in unrealistic flow simulation.

   In this study, a numerical method has been applied for the simulation of fluid flows in the two- and three-dimensional tanks. The global fluid motion is of interest and local nonlinear phenomena are not considered in detail. The method of solution is a finite difference method, adopting staggered grids. The free surface profile is assumed to be single-valued, so that SURF scheme is applicable to the numerical implementation of free-surface boundary condition. The numerical computation has been carried out for a few models which experimental or other computational results are available. The present results include the computation of impact pressure on tank ceiling. Moreover, the developed computer program was extended to the real-ship application.

Numerical Method

   The present study adopts SOLA method for the Navier-Stokes equation. This method is well known, and the details can be found in [3]. In this method, the finite-difference form of the velocity vector in the $(n+1)$-th time step, $\vec{u}_{ijk}^{(n+1)}$, can be written as follows:

$$\vec{u}_{ijk}^{(n+1)} = \vec{u}_{ijk}^{*} + \Delta p_{ijk} \frac{\Delta t}{\Delta(x,y,z)}$$

where

$$\vec{u}_{ijk}^{*} = \vec{u}_{ijk}^{(n)} + \Delta t \left[-\frac{1}{\rho}(\hat{\nabla}p)_{ijk}^{(n)} + \nu\,(\hat{\nabla}^2\vec{u})_{ijk}^{(n)} + (\vec{f})_{ijk}^{(n+1)} \right] - \Delta t \{ \vec{u} \cdot \hat{\nabla} \}_{ijk}^{(n)} \vec{u}_{ijk}^{(n)} \}$$

$$\Delta p_{i,j,k} = -\frac{(\hat{\nabla} \cdot \vec{u}_{ijk}^{*})}{2\Delta t\left(1/\Delta x^2 + 1/\Delta y^2 + 1/\Delta z^2\right)}$$

and $\rho, \nu, p, \vec{f}$ are the liquid density , kinemtaic viscosity, pressure and external force vectors, respectively. Here, the three-dimensional staggered grids are distributed in whole tank domain, and the subscript i,j,k indicates the cell index. In the present study, a conservative form of the mixed central-upwind difference is applied for the convection term in the Navier-Stokes equation.

   The free surface elevation can be obtained from the kinematic condition which takes the following form:

$$\eta_{ij}^{(n+1)} = \eta_{ij}^{(n)} + \Delta t \left[w - u\frac{\partial \eta}{\partial x} - v\frac{\partial \eta}{\partial y} \right]_{ij}$$

The dynamic condition can be imposed using the irregular-star method. In this method, the pressure at the cell near free surface is interpolated from the pressure values at six neighbor points, including the points on free surface.

A no-slip condition is valid when the viscous effect is so significant that the boundary layer thickness is comparable to the cell size. However, generally, the viscous does not influence much on violent sloshing flow. In this study, a free-slip condition is applied on tank walls.

Impact Pressure Computation

Some spectial numerical treatments are required when the liquid contacts tank ceiling or horizontal members. First of all, the detachment of fluid from ceiling should be properly simulated. When a part of fluid is on the tank top, a typical no-flux condition tends to prevent the vertical detachment. In the present computation, the downward velocity is allowed at the tank top boundary if the free surface is nearby and moves down. In a LNG cargo, the downward velocity should be also allowed when the preseure is less than the vapor pressure.

As pointed in some studies, the typical wall condition on the tank top can produce too large impact pressure. This study adopts the concept of buffer zone, which has been successfully applied by Mikelis and some Japanease. In the buffer zone near the tank top, the free-surface boundary condition is modified to the following form:

$$\kappa \frac{p_f - p_{atm}}{\rho} - (1-\kappa) \frac{H_B}{\Delta t} w_f = 0$$

where

$$\kappa = \begin{bmatrix} (D-\eta)/H_B & D - H_B \leq \eta < D \\ 0 & \eta \leq D - H_B \\ 1 & \eta = D \end{bmatrix}.$$

D is the tank depth and H_B is the size of buffer zone. This is the linear combination of the no-flux wall condition and dynamic free surface condition. Therefore, the existance of wall boundary affects on the fluid motion when the free surface is inside the buffer zone. This condition is valid only when the free surface moves upward. In the real physical phenomenon, the magnitude of impact pressure depends on some other factors, like the air cushion, structural response and liquid compressibility. The concept of buffer zone may reflect a part of such effects during an impact occurs.

Averaging the signal over several time steps is an another numerical treatment for the impulsive dynamic pressure. Since the finite number of cells are used in the numerical computation, the computational pressure signal shows the series of discrete impulses. According to the computational experience, the averaged signal shows closer time-history and peak than not-averged results.

The classical criterias for the numerical stability are valid in the present study. For example, the Courant condition for the velocity and wave should be satisfied. In addition, it is desirable that the time segment should be fine enough for the free surface to experience the boundary condition in the buffer zone.

Computational Results

In the numerical computation, the upwinding factor for the convection term was fixed to be 0.75 and the kinematic viscosity has been set to be $10^{-6}\text{m}^2/\text{sec}$. For the two-dimensional computation, only one mesh sheet was distributed along the transverse direction.

Figure 1 shows a comparison of the instantaneous wave elevation with the linear analytic solution. When a small amplitude excitation with an out-of-resonance frequency, the numerical solution is very close to the analytic solution. In the case of Figure 1, the excitation is near resonance, so that a typical difference between the nonlinear and linear results can be observed.

Figure 2 shows an instantaneous snapshot of fluid motion, and it is compared with experiment. This tank has the same dimensions with Figure 1, but one deep vertical baffle and three horizontal members are in the tank. The experimental result is from [4]. From this figure, we can figure out that the present method provides quite reasonable solution even for a tank with internal members.

Figure 3 shows the computed pressure signals with different meshes. The observation points are the center of corner cells between the tank top and side wall. Generally the larger impact pressure is generated when the mesh size becomes smaller, but it should be noticed that the averaged signals do not show a significant discrepancy.
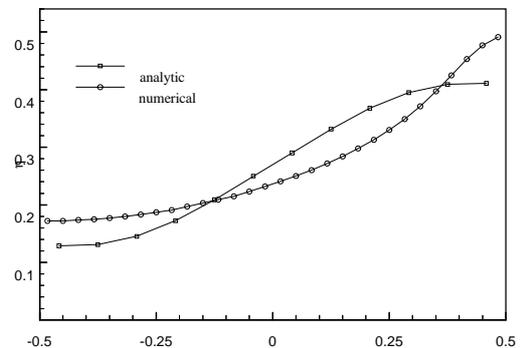

Figure 1. Instantaneous surface profile; 0.8m(L)×0.8m(B)×0.54m(D), 50% filling, T_1=1.15sec, A_1=0.01m, 30x1x20 meshes, no internal members, t=5.4 sec

Figure 4 shows the comparison of the computed and measured pressure signals on the tank top. The measurement shows unsteady peaks, but the maximum pressure is close to the numerical result. According to the computational experience, averaging over 4~6 time steps provides reasonable results.
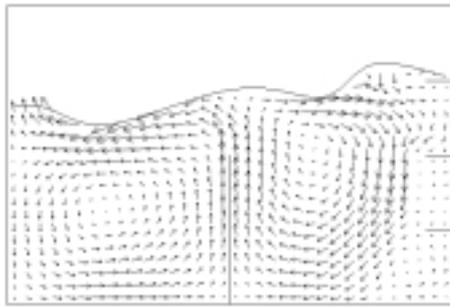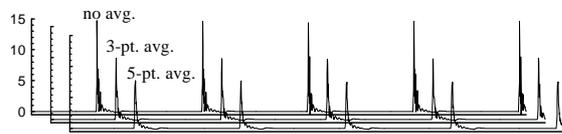

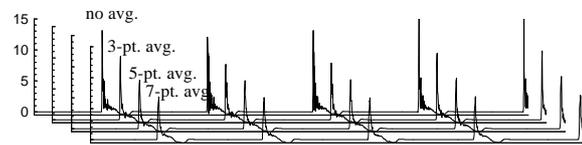(a) Computed velocity vectors and elevation
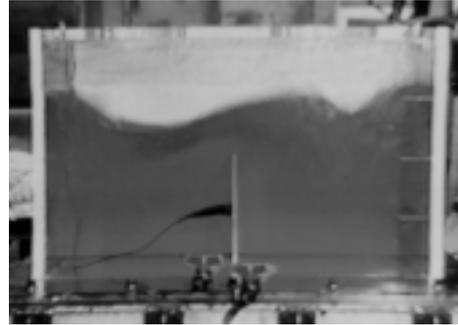
(b) Experiment

Figure 2. Instantaneous snapshots of fluid motion; the same dimension with Figure 1, 70% filling, T_1=1.08sec, A_1=0.04m, 30x1x20 meshes, with internal members

(a) 30 x 20

(b) 40 x 30

Figure 3. Grid dependency of the pressure signal at tank top; the same tank with Figure 1, 80% filling, T_1=1.175sec, A_1=0.04m, 5.5sec time window, H_B=0.5Δz, peak of experimental data: 9.07kN/m^2

Figure 5 shows the wave profile in a three-dimensional tank, and the tank dimension and excitation conditions are the same with those of [6]. In this case, the excitation frequency is the third mode of natural motion, and both surge and sway motions are under the excitation. The z-coordinate is scaled for the comparison with their result (small figure), and two results show a good agreement.
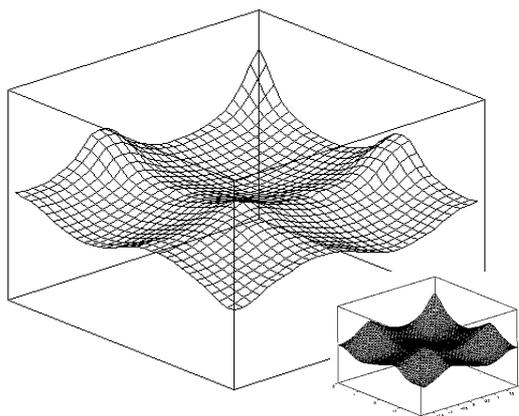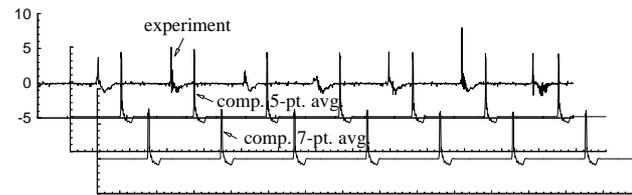

Figure 4. Pressure time-histories on tank top; the same tank with Figure 1, 70% filling, T_1=0.98sec, A_1=0.038m, 30×1× 20 meshes, H =0.5Δz

Figure 5. Instantaneous wave profile in a 3-D tank; L/d=B/d=4, $T_1\sqrt{g/d}=$ $T_2\sqrt{g/d}$ =4.13, A_1/d=A_2/d= 0.0186, 30×30×30 meshes (small figure; Wu, Ma & Taylor[6])
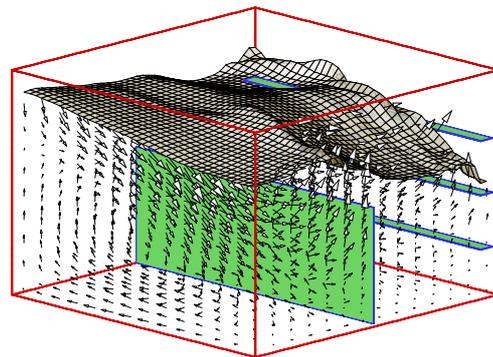

Figure 6. Instantaneous wave profile and velocity vectors in a 3-D tank; the same tank with Figure 2, B=0.8m, T_4=T_5=1.30sec, A_4=A_5=4deg., 40×40×30 meshes

Figure 6 shows the instantaneous surface profile and velocity vectors on fluid domain when the tank is under the roll and pitch excitations. The fluid motion in this tank is complicated because of the internal members.

Especially, the deep vertical member plays an important role to block the horizontal motion.

Figure 7 shows the wave elevation at two tank corners of the same side when the roll motion is under excitation. In this case, the horizontal members influence on the fluid motion in some region, resulting in the three-dimensional flows. Therefore, we can observe some time-delay of the pressure impulse at the left and right corners. This is an another effect of the horizontal member, which is different with Figure 2. In this figure, the flat crests indicate that the fluid contacts the tank ceiling, and other flat signals are due to the horizontal member.

Figure 8 shows the pressure history at a corner of tank top when the tank is under both surge and sway excitations. In particular, two motions have the same frequency and amplitude but the phase difference is applied in the case of Figure (b). In this case, the 45-deg. phase difference induces the rotational surface motion. Therefore, the impact area on the tank top turns around periodically along the top edges, and the maximum pressure is much less than the case without phase difference.

The present computation is extended to multi-tank sloshing analysis for real ships. Figure 9 shows an application example for a LNG carrier with five tanks. In the real-ship computation, it is desirable to couple a ship-motion program with the sloshing analysis code since the sloshing-induced forces and moments affect on the ship motion. A study for coupling with the three-dimensional ship-motion program is in progress.
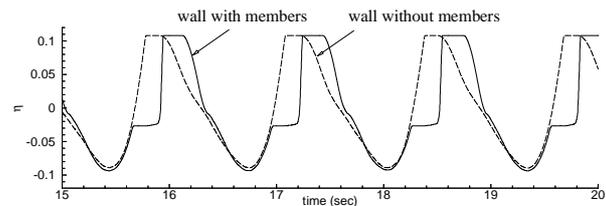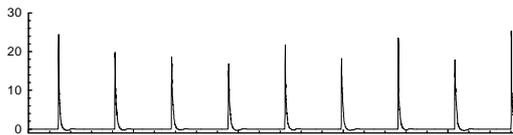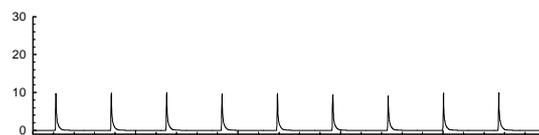

Figure 7. Surface elevation at two corners; the same tank with Figure 2; 80% filling, $T_4=1.30$sec, $A_4=4$deg.

(a) No phase difference

(b) 45° phase difference

Figure 8. Time histories of pressure on a ceiling corner; $T_1=T_2=1.08$sec, 45° phase difference, $A_1=A_2=0.02$m, $30\times30\times20$ meshes, x/L=y/B=0.983, 5-pt. averaged
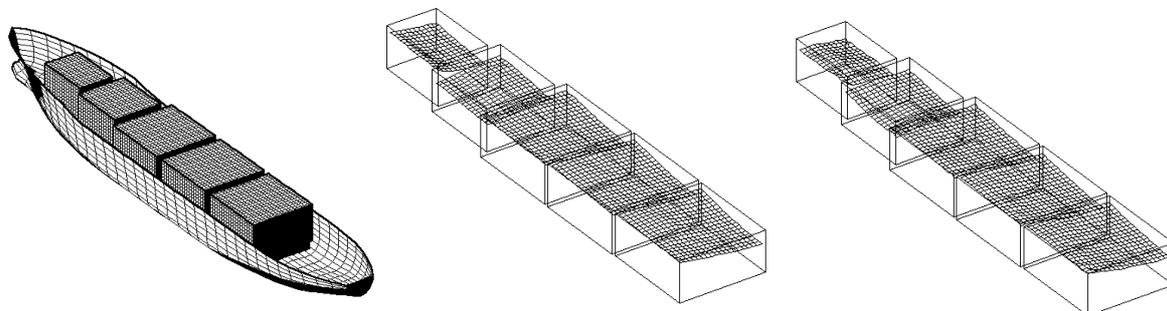

Figure 9. Sloshing in a LNG carrier; LAMP modeling for motion, sway-heave-roll-pitch coupling

Acknowledgement

References

[1] Bridges, T.J., 1982, 'A numerical simulation of large amplitude sloshing', *Proc. of the 3rd International Numerical Ship Hydrodynamics*

[2] Faltinsen, O.M., 1978, 'A numerical non-linear method of sloshing in tanks with two dimensional flow', *Journal of Ship Research*, Vol.18

[3] Hirt, C.W. & et al, 1975, 'SOLA-A numerical solution algorithm for transient fluid flows', *Report LA-5852*, Los Alamos Scientific Laboratory

[4] Kim, Y., 1993, 'Development of sloshing analysis system, II', DAEWOO HMI, *Research Report SH-9121*

[5] Mikelis & et al, 1984, 'Sloshing in partially filled liquid tanks and its effect on ship motions', *Trans. Of RINA*, Vol.126

[6] Wu, G.X. and et al, 1998, 'Numerical simulation of sloshing waves in a 3D tank based on a finite element method', *Applied Ocean Research*, Vol.20